Inorg. Chem. **2006**, *45*, 5607–5616

Iron(III) Coordination Properties of a Pyoverdin Siderophore Produced by *Pseudomonas putida* ATCC 33015

Hakim Boukhalfa,[†] Sean D. Reilly,[†] Ryszard Michalczyk,[‡] Srinivas Iyer,[‡] and Mary P. Neu*[,†]

Chemistry Division and Bioscience Division, Los Alamos National Laboratory, Los Alamos, New Mexico 87545

Received February 3, 2006

The iron complexation of a fluorescent green pyoverdin siderophore produced by the environmental bacterium *Pseudomonas putida* was characterized by solution thermodynamic methods. Pyoverdin binds iron through three bidentate chelate groups, a catecholate, a hydroxamate, and an α-hydroxycarboxylic acid. The deprotonation constants of the free pyoverdin and Fe(III)–pyoverdin complex were determined through a series of potentiometric and spectrophotometric experiments. The ferric complex of pyoverdin forms at very low pH (pH < 2), but full iron coordination does not occur until neutral pH. The calculated pM value of 25.13 is slightly lower than that for pyoverdin PaA (pM = 27), which coordinates iron by a catecholate and two hydroxamate groups. The redox potential of Fe–pyoverdin was found to be very pH sensitive. At high pH (∼pH 9–11) where pyoverdin coordinates Fe in a hexadentate mode the redox potential is –0.480 V (NHE); however, at neutral pH where full Fe coordination is incomplete, the redox potential is more positive ($E_{1/2}$ = –0.395 V). The positive shift in the redox potential and the partial dissociation of the Fe–pyoverdin complex with pH decrease provides a path toward in vivo iron release.

Introduction

Iron is an essential nutrient for almost all living organisms. Although abundant in nature, iron generally exists in forms that render it unavailable to microorganisms. Under oxic conditions, the low solubility of iron hydroxyl polymers limits the aqueous concentration of Fe(III) to 10^{-10} M,[1,2] significantly below the concentration required to meet the cell's optimal iron needs of 10^5-10^6 ions per bacterial cell.[3,4] Pathogenic bacteria face a similar challenge in acquiring nutrient iron from their host, where the iron is bound to high-affinity proteins, such as ferritins, hemes, and transferrins.[5] Microbial Fe(III) acquisition therefore requires competitive and selective iron binding outside the cell and its transport across the cell membrane. Most bacteria produce low-molecular-weight chelators, called siderophores, to sequester iron and mediate nutrient iron transport across the cell membrane through a selective Fe(III)−siderophore transport system.[6−9]

Among the many natural siderophores identified,[10] pyoverdins constitute a distinctive class that have unique structural and fluorescence features. Pyoverdins are comprised of a peptide chain and a fluorescent multifunctional chromophore, 2,3-diamino-6,7-dihydroxyquinoline.[11−14] Both the peptide chain and chromophore vary slightly in composition, depending upon the bacterial strain and the growth medium constituents.[12] In addition to these general features,

* To whom correspondence should be addressed. E-mail: mneu@lanl.gov. Phone: 505-667-7717.
[†] Chemistry Division.
[‡] Bioscience Division.

(1) Chipperfield, J. R.; Ratledge, C. *BioMetals* **2000**, *13*, 165−168.
(2) Boukhalfa, H.; Crumbliss, A. L. *BioMetals* **2002**, *15*, 325−339.
(3) Braun, V.; Killmann, H. *Trends Biochem. Sci.* **1999**, *24*, 104−109.
(4) Volkmar, B.; Klaus, H. In *Microbial Transport Systems*; Winkelmann, G., Ed.; Wiley-VCH: Weinheim, Germany, 2001; pp 289−311.
(5) Braun, V.; Hantke, K.; Köster, W. In *Metal Ions in Biological Systems*; Sigel, A., Sigel, H., Eds.; Marcel Dekker: New York, 1998; Vol. 35, pp 67−145.
(6) Neilands, J. B. *J. Bio. Chem.* **1995**, *270*, 26723−26726.
(7) Brown, C. M.; Trick, C. G. *Arch. Microbiol.* **1992**, *157*, 349−354.
(8) Stintzi, A.; Barnes, C.; Xu, J.; Raymond, K. N. *Proc. Natl. Acad. Sci. U.S.A.* **2000**, *97*, 10691−10696.
(9) Folschweiller, N.; Schalk, I. J.; Celia, H.; Kieffer, B.; Abdallah, M. A.; Pattus, F. *Mol. Membr. Biol.* **2000**, *17*, 123−133.
(10) Ratledge, C.; Dover, L. G. *Annu. Rev. Microbiol.* **2000**, *54*, 881−941.
(11) Kilz, S.; Lenz, C.; Fuchs, R.; Budzikiewicz, H. *J. Mass Spectrom.* **1999**, *34*, 281−290.
(12) Fuchs, R.; Budzikiewicz, H. *Curr. Org. Chem.* **2001**, *5*, 265−288.
(13) Demange, P.; Bateman, A.; Mertz, C.; Dell, A.; Piemont, Y.; Abdallah, M. A. *Biochemistry* **1990**, *29*, 11041−11051.
(14) Wasielewski, E.; Atkinson, R. A.; Abdallah, M. A.; Kieffer, B. *Biochemistry* **2002**, *41*, 12488−12497.

10.1021/ic060196p CCC: $33.50
Published on Web 06/17/2006

pyoverdins contain three bidentate metal-binding functional groups: a catecholate group within the 2,3-diamino-6,7-dihydroxyquinoline chromophore, a hydroxamate group at the end of the peptidic chain, and either a second hydroxamate or an α-hydroxycarboxylic group in the middle of the peptidic chain. Although more than 50 different pyoverdins or pyoverdin-like siderophores have been structurally characterized, the iron-chelation properties have been studied for only a few pyoverdins.[15−17]

In this paper, we report the structural characterization and complete solution thermodynamics of a pyoverdin siderophore produced by *Pseudomonas putida* strain ATCC 33015. This bacterium, commonly found in soils, plays an important role in Mn(II) oxidation,[18] direct or indirect metal reduction/oxidation,[19,20] and the degradation of aromatic compounds.[21] The structure of the pyoverdin is comprised of a succinic acid 2,3-diamino-6,7-dihydroxyquinoline chromophore and a peptidic chain with the following seven amino acids: Asp−Orn−OHAsp−Dab−Gly−Ser−cOHOrn. The free pyoverdin has nine deprotonation sites; five deprotonation sites within three bidentate iron binding units, three deprotonation sites on the peptide chain not involved in iron chelation, and a deprotonation site on the side chain attached to the chromophore. The structure of this pyoverdin siderophore is similar to that of the siderophore produced by *P. putida* G4R.[22] The formation of the ferric complex in highly acidic solution (pH < 2) and the sequential deprotonation of the complex formed at higher pH were studied through a series of potentiometric and spectrophotometric measurements. The redox behavior of the pyoverdin−iron complex was investigated by cyclic voltammetry. Data from this study are compared to those pertaining to the coordination properties of other siderophores, such as pyoverdin PaA[15] and azotobactor.[16]

Experimental Section

Bacterial Strain and Culture Conditions. *P. putida* strain ATCC 33015 was purchased from the American Type Culture Collection. The growth media composition per liter is 0.67 g of glycerol-2-phosphate, 1.0 g of NH_4Cl, 0.2 g of $MgSO_4 \cdot 7H_2O$, 0.05 g of $CaCl_2$, 0.5 g of KCl, 5.0 g of succinic acid, trace elements 0.125 mL. Trace metals were added from a stock solution containing a 1000 × fold stock of 97.7 g of $MgSO_4$ per liter, and a 1000 × trace element solution (70 mg of $CuSO_4$, 35 mg of $MnSO_4 \cdot H_2O$, 23.7 mg of $ZnCl_2$, 1000 mg of $CaCl_2$, 18 mg of $CoCl_2$, 7 mg of H_3BO_3, and 60 mg of $(NH_4)_6Mo_7O_{24} \cdot 4H_2O$ per liter), and $FeSO_4 \cdot 7H_2O$. For siderophore production, the media was treated with a Chelex 100 resin (Sigma) to remove all residual metals prior to the addition of the trace metals solution. The bacteria were grown at 30 °C in 4-L acid-washed and autoclaved, conical glass flasks maintained in the dark under constant shaking at 160 rpm.

Pyoverdin Production and Purification. Pyoverdin was isolated from a 4-day-old culture of *P. putida* cultured under iron-deficient conditions. The culture media was isolated from the cells by centrifugation at 5000 rpm for 15 min at 4 °C and filtration using polycarbonate 0.20-μm-pore-size filters. The crude culture extracts were concentrated by rotary evaporation and adjusted to pH 5 by the addition of acetic acid. Pyoverdin was initially purified from the concentrated culture media by preparative chromatography using a variation of the purification protocol previously described in the literature.[13,23] Pure fractions of the main pyoverdin produced were isolated by preparative chromatography using a reverse-phase C-18 Lichroprep 40−63-μm Merck column. The column (1:20 cm) was prepared in acetonitrile and equilibrated with a pH 5 acetate buffer solution. The crude siderophore at pH 5 was applied to the column and washed with four volumes of the acetate buffer and eluted with a 5:95 v/v mixture of acetonitrile/acetate buffer. The fractions of pure pyoverdin eluted were evaporated to dryness, lyophilized, and stored at −20 °C. ^{15}N-labeled siderophore was generated by the replacement of $^{14}NH_4Cl$ with $^{15}NH_4Cl$ in the growth media. Pyoverdin was also purified as a gallium complex following the same procedure. The gallium complex was formed by addition of excess gallium acetate to the crude siderophore. The purification procedure was the same as for the free pyoverdin. All glassware used were acid-washed in a 50:50 (v/v) mixture of concentrated sulfuric and nitric acid for a minimum of 1 h to remove any traces of iron and rinsed repeatedly with double-distilled water.

Mass Spectrometry Analysis. Pyoverdin samples were mixed 1:1 with α-cyano-4-hydroxycinnamic acid in 50% acetonitrile/0.1% TFA (trifluoroacetic acid) and spotted on 100-well stainless steel probes. MALDI-MS analysis was performed using a Voyager DE-STR (Applied Biosystems) in positive ion, reflector mode using angiotensin II as a single-point external calibrant. When desired, post source decay (PSD) analysis[24] was performed using a multi-point calibration generated with a PSD spectrum of angiotensin. Composite PSD spectra were stitched using the Data Explorer software.

NMR Spectroscopy. ^1H, ^{13}C, and ^{15}N NMR spectra were collected on a Bruker DRX-500 instrument equipped with a triple-resonance probe and triple axis gradients. All spectra were recorded in DMSO-d_6, and the solvent signal was used as an internal reference for all ^1H and ^{13}C spectra; ^{15}N spectra were referenced to liquid ammonia (0.00 ppm) through the lock frequency. All spectra were recorded at 298 K.

1D ^1H spectra were obtained using a standard one-pulse sequence. ^{13}C and ^{15}N proton-decoupled spectra were obtained using the inverse gated pulse program with WALTZ-16 decoupling during acquisition. CH, NH, CH_2, and NH_2 groups were assigned using DEPT spectra with flip angles of 45° and 90° and WALTZ-16 proton decoupling. Through-bond ^1H correlations were obtained using 2D Double-Quantum-Filtered (DQF) COSY spectra and TOCSY spectra collected with 12.5, 25, and 50 ms mixing time. Spectral width in the experiments was set to 6 kHz in both dimensions, and the spectra were collected with 2048 complex

(15) Albrecht-Gary, A. M.; Blanc, S.; Rochel, N.; Ocaktan, A. Z.; Abdallah, M. A. *Inorg. Chem.* **1994**, *33*, 6391−6402.
(16) Palanche, T.; Blanc, S.; Hennard, C.; Abdallah, M. A.; Albrecht-Gary, A. M. *Inorg. Chem.* **2004**, *43*, 1137−1152.
(17) Parker, D. L.; Sposito, G.; Tebo, B. M. *Geochim. Cosmochim. Acta* **2004**, *68*, 4809−4820.
(18) Tebo, B. M.; Bargar, J. R.; Clement, B. G.; Dick, G. J.; Murray, K. J.; Parker, D.; Verity, R.; Webb, S. M. *Annu. Rev. Earth Planet. Sci.* **2004**, *32*, 287−328.
(19) Ishibashi, Y.; Cervantes, C.; Silver, S. *Appl. Environ. Microbiol.* **1990**, *56*, 2268−2270.
(20) Murray, K. J.; Mozafarzadeh, M. L.; Tebo, B. M. *Geomicrobiol. J.* **2005**, *22*, 151−159.
(21) Ganguli, A.; Tripathi, A. *Appl. Microbiol. Biotechnol.* **2002**, *58*, 416−420.
(22) Salah El Din, A. L. M.; Kyslik, P.; Stephan, D.; Abdallah, M. A. *Tetrahedron* **1997**, *53*, 12539−12552.
(23) Teintze, M.; Hossain, M. B.; Barnes, C. L.; Leong, J.; Van der Helm, D. *Biochemistry* **1981**, *20*, 6446−6457.
(24) Kaufmann, R.; Kirsch, D.; Spengler, B. *Int. J. Mass Spectrom. Ion Processes* **1994**, *131*, 355−385.

points in the direct dimension and 512 complex points in the indirect dimension. Quadrature detection in t_1 was achieved using the TPPI method. ^{15}N-decouping was achieved with a 180° pulse during the t_1 period and with WALTZ-16 decoupling sequence during acquisition. For TOCSY spectra a DIPSI-2 mixing sequence was used with 6.75-kHz radiofrequency field. 2D NOESY spectra were recorded using the pulse sequence with gradient selection and ^{15}N-decoupling (180° pulse during the t_1 period and WALTZ-16 decoupling sequence during acquisition). Spectra were obtained at 50, 100, and 200 ms mixing times, with 6-kHz spectral width in both dimensions and 2048 × 512 complex points. Quadrature detection in t_1 was achieved using TPPI method. Assignment of ^{13}C resonances was obtained from ^{1}H−^{13}C HSQC and long-range (LR) HSQC spectra. Spectra were recorded using a pulse sequence with echo−antiecho gradient selection. Spectral width was set to 6 kHz in the ^{1}H dimension and 17.6 kHz in the ^{13}C dimension (21 kHz for LR-HSQC), with 2048 and 256 complex points, respectively. The INEPT transfer delay was set to 1.72 ms for HSQC and 16.6 ms for LR-HSQC experiments, and the spectra were collected with 96 and 320 scans per t_1 increment, respectively. The one-bond INEPT transfer was not suppressed in the LR-HSQC experiment. Assignment of ^{15}N resonances was obtained from ^{1}H−^{15}N HSQC and LR-HSQC spectra. Spectra were recorded using a pulse sequence with an echo−antiecho gradient selection. Spectral width was set to 6 kHz in the ^{1}H dimension and 3.2 kHz in the ^{15}N dimension, with 2048 and 128 complex points, respectively. The INEPT transfer delay was set to 2.7 ms for HSQC and 16.6 ms for LR-HSQC experiments, and the spectra were collected with 96 and 256 scans per t_1 increment, respectively. The one-bond INEPT transfer was not suppressed in the LR-HSQC experiment.

Potentiometric and Spectrophotometric Measurements. The solutions were prepared with deionized water, and the ionic strength was fixed at 0.10 M using sodium nitrate. The ferric nitrate stock solution used to prepare all the ferric pyoverdin complexes that were analyzed spectrophotometrically was prepared from ferric nitrate salt dissolved in 1.0 M nitric acid (HNO_3) and standardized using a graphite furnace atomic absorption spectrometer. The ferric solution used for potentiometric titrations was a commercial 0.0180-(1) M ferric nitrate standard solution (from High-Purity Standards, Inc). The initial concentrations of pyoverdin were calculated using the extinction coefficient $\epsilon_{377} = 12670\ M^{-1}\ cm^{-1}$ for the free pyoverdin at pH 5.0. This extinction coefficient was determined from an aqueous solution whose iron concentration was determined using a graphite furnace atomic absorption spectrometer (GFAA). All potentiometric measurements were conducted on stirred solutions in a water-jacketed vessel at 25.0 ± 0.1 °C under ultrapure argon atmosphere. Titrants were dispensed using a Brinkmann Metrohm 665 Dosimat. Potentiometric measurements were made using an Orion Research EA940 pH meter and an Orion ROSS combination pH electrode filled with 3.0 M aqueous sodium nitrate. The pH electrode was calibrated by an acid−base titration before each experiment such that $-\log [H^+]$ was measured directly. The titration of pyoverdin (0.01997 mmol, pH 2.54−11.19) was performed by incremental addition (0.05 mL) of standardized sodium hydroxide (NaOH, 0.1014(3) M) to the ligand solution maintained under argon and constant stirring. The titration of the Fe(III)−pyoverdin complex (0.02086 mmol of pyoverdin and 0.02088 mmol of Fe(III), pH 1.80−11.39) was performed similarly. Experimental data were modeled numerically using the program SUPERQUAD.[25] The Fe(III), pyoverdin, and free proton concentrations were refined along with the stability constants. The initial free proton concentrations were estimated from the amounts of acid contained in the ferric nitrate added. The differences between the Fe(III) and pyoverdin concentrations calculated and refined from the pH data were less than 5%. All UV−visible spectra were measured at 25 °C in a quartz cuvette with a 1.0-cm path length and recorded using a Varian Cary 6000i spectrophotometer. The pH measurements for spectrophotometric titrations between pH 3.67 and 8.67 were made using a Fisher Scientific AR 15 pH meter equipped with an Orion ROSS semi-micro combination electrode filled with a 3.0 M KCl solution. The pH meter was calibrated to read the pH value using commercial Fisher buffered solutions (pH = 4.00, 7.00, and 10.00). The pH values for spectrophotometric titrations between pH 9.38 and 13.48 were calculated from the amounts of base added. The UV−visible titration of free pyoverdin was performed by incremental addition of known volumes of standardized sodium hydroxide (NaOH, 0.98 and 2.0 M) to the ligand solution maintained under constant stirring. The spectrum of free pyoverdin was recorded at each pH when equilibrium was reached. The titration of the Fe(III)−pyoverdin complex ([Fe(III)] = 0.054×10^{-6} M and [pyoverdin] = 0.055×10^{-6} M) was performed similarly between pH 2.61 and 7.52. Under more acidic conditions, solutions containing 0.054×10^{-6} M Fe(III), 0.055×10^{-6} M pyoverdin, and proton concentrations varying from 0.010 to 0.10 M were equilibrated for 30 min and their UV−visible spectra were recorded. The proton concentrations were calculated from the amounts of acid added. Data were analyzed to determine equilibrium constants using the program LETAGROP-SPEFO.[26]

Electrochemistry. Cyclic voltammetry measurements were performed using a bi-potentiostat−galvanostat model INCCHI700B from Chinstruments, Inc. All cyclic voltammetry measurements were made in argon-saturated deionized water using a conventional three electrode cell: BAS model MF-2052 reference electrode Ag/AgCl filled with a 3 M NaCl solution and saturated with AgCl, platinum wire auxiliary electrode, and a PAR G0021 platinum working electrode (0.28 mm^2 surface area). A small-volume cell (3 mL) was used for all measurements. The Fe(III)−pyoverdin concentration was 2.0 mM. The working electrode was smoothly polished using a 0.5-μm alumina polish for 2 min and cleaned with distilled water prior to each measurement. The Fe(III)−pyoverdin complex solutions were prepared by adding 1 equiv of Fe(III) from an acidic stock solution to a pyoverdin solution (pH 3.5). The ionic strength was adjusted to $I = 0.10$ M by the addition of aqueous 1.0 M sodium nitrate ($NaNO_3$). Cyclic voltammograms were recorded between 0.0 and −0.90 V at a scan rate of 60 mV/s. The pH of the Fe(III)−pyoverdin complex solution was adjusted by addition of NaOH and measured using a Fisher Scientific AR 15 pH meter equipped with an Orion ROSS semi-micro combination electrode filled with a 3 M NaCl solution.

Results and Discussion

1. Bacterial Growth Conditions and Pyoverdin Purification. *P. putida* culture was grown on a succinic medium under iron-limited conditions. To eliminate iron contamination, all flasks used for media preparation were acid-washed and the media were passed through a cation-exchange resin to remove residual iron. The cell density at full growth under iron deprivation reached optical densities at 600 nm of 0.7−0.9. The major siderophore (pyoverdin) production (60%)

(25) Gans, P.; Sabatini, A.; Vacca, A. *J. Chem. Soc., Dalton Trans.* **1985**, 1195−1200.

(26) Raymond, K. N.; Müller, G.; Matzanke, B. F. In *Topics in Current Chemistry*; Boscheke, F. L., Eds.; Springer-Verlag: New York, 1984; Vol. 123, pp 49−102.

Table 1. ^{1}H NMR Chemical Shifts (ppm) and Assignments for the Spectrum of Ga(III)−pyoverdin in DMSO-d_6

succinic acid	C^{1}O	α	β	C^{4}O									
		2.618	2.552										
chromophore	NH	2	3	4	5	6	7	8	9	10	11	12	13
	8.270	−	−	7.676	6.739	−	−	6.459	−	−	5.605	2.501, 2.165	3.511, 3.071
amino acids	NH	α	β	γ	δ	NH_2							
Asp	8.904	4.721	2.711										
Orn	8.820	4.128	1.762	1.758	3.248	7.536							
				1.564	2.807	6.961							
OHAsp	9.433	4.901	4.710										
Dab	10.159	4.107	1.990	3.029		7.59							
			1.764										
Gly	9.730	4.336											
		3.887											
Ser	8.156	4.234	3.665										
cOHOrn	7.747	4.418	1.973	1.774	3.498								
			1.723		3.234								

Table 2. ^{13}C NMR Chemical Shifts (ppm) and Assignments for the Spectrum of Ga(III)−pyoverdin in DMSO-d_6

succinic acid	CO	COOH	α	β	NH								
	174.20	174.12	30.53	29.20	9.550								
chromophore	CO	2	3	4	5	6	7	8	9	10	11	12	13
	169.00	146.41	113.65	136.36	106.14	163.08	155.26	96.60	130.68	113.51	55.62	22.72	35.04
amino acids	CO	α	β	γ	δ								
Asp	170.02	48.66	35.95										
Orn	172.02	54.28	26.18	22.02	37.88								
OHAsp	163.19	54.64	74.05										
Dab	169.13	51.02	20.13	35.59									
Gly	167.02	41.06											
Ser	171.09	56.94	60.94										
OHOrn	160.45	47.41	27.17	19.36	49.98								

occurred in the first 4 days following the culture inoculation. The total amount of pyoverdin produced in 4 days ranged from 100 to 300 mg/L. Pyoverdin was purified from the growth media by preparative chromatography using a C-18 reverse-phase column. Pyoverdin was also purified as a Ga(III)−pyoverdin complex following the same procedure. Free pyoverdin was subsequently obtained from the Ga(III)−pyoverdin complex by EDTA dechelation followed by chromatography purification on a C-18 reversed-phase column.

2. Pyoverdin Structure. The molecular mass of the main pyoverdin produced by this bacterium was obtained by MALDI-TOF analysis of the crude extracts obtained from cultures grown under iron-deficient conditions. The mass spectrum shows a molecular ion peak at $m/z = 1092$ for the main peak and a minor peak at (M − 18) $m/z = 1075$. The primary structure was determined using ^{1}H, ^{13}C, and ^{15}N NMR studies of the ^{15}N-labeled Ga(III)−pyoverdin complex and was confirmed by mass spectrometry fragmentation of the free pyoverdin obtained by MALDI−PSD analysis.

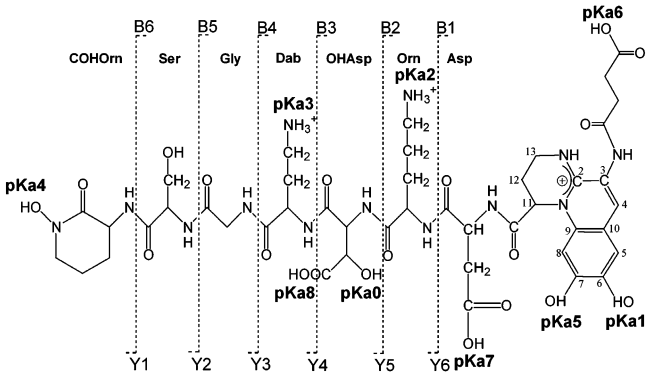

Figure 1. Molecular structure of a pyoverdin, siderophore isolated from *Pseudomonas putida* ATCC 33015. Bn and Yn refer to N-terminal and C-terminal fragments.

2.1. NMR Studies of ^{15}N-Labeled Ga(III)−Pyoverdin Complex. The aliphatic and chromophore proton and carbon resonances were assigned from NOESY, ^{1}H−^{13}C HSQC, and LR-HSQC spectra. H11 at 5.605 ppm is easily identified as the only hydrogen showing a NOESY cross-peak to the peptide NH group of Asp-1 (see Figure 1 for chromophore atom numbering). The TOCSY cross-peaks from H11 identify H12 and H13 hydrogens (2.165−2.501 and 3.071−3.511 ppm, respectively). The chromophore contains three aromatic hydrogens—H4, H5, and H8. The NOESY cross-peak between H11 at 5.605 ppm and a proton resonance at 6.459 ppm clearly assigns the latter to H8 of the chromophore. Similarly, the cross-peak between the NH group of the succinyl side chain to the proton at 7.676 ppm assigns it to H4 of the chromophore. The remaining aromatic proton at 6.739 ppm shows a NOESY cross-peak to H4 and is assigned to hydrogen H5 of the chromophore. The chemical shifts of these three aromatic protons are slightly shifted compared to their analogous protons in the structure of pyoverdin G4R[22] observed at 7.90, 7.15, and 6.95 ppm. This shift is due to the utilization of a different solvent and also to gallium binding, which is expected to affect the protons close to the gallium binding sites. Analysis of ^{1}H−^{13}C HSQC spectrum easily identifies the carbons bound to the assigned hydrogens of the chromophore (Tables 1 and 2). Similarly, cross-peaks in the ^{1}H−^{13}C LR-HSQC spectra clearly identify the remaining quaternary carbons. The ^{1}H and ^{13}C chemical

Table 3. List of *m*/*z* Fragments of *P. Putida* Pyoverdin Siderophore Obtained by MALDI−PSD Fragmentation and Their Assignments

unlabeled pyoverdin *m*/*z*	^{15}N-labeled pyoverdin *m*/*z*	C vs N	assignment of C and N-terminal fragments
357.6	361.7	B0	Suc−Chr
472.8	477.5	B1	Suc−Chr−Asp
587.5	594.3	B2	Suc−Chr−Asp−Orn
718.7	725.6	B3	Suc−Chr−Asp−Orn−OHAsp
817.8	827.7	B4	Suc−Chr−Asp−Orn−OHAsp−Dab
275.2	280.3	Y3	Gly−Ser−cOHOrn
373.6	379.8	Y4	Dab−Gly−Ser−cOHOrn
646.7	654.1	Y6	CO−NH−Orn−OHAsp−Dab−Gly−Ser−cOHOrn
744.8	753.6	Y6	CO−Asp−Orn−OHAsp−Dab−Gly−Ser−cOHOrn
1092.1 (M+)	1105.7(M+)		Suc−Chr−Asp−Orn−OHAsp−Dab−Gly−Ser−cOHOrn

shifts measured and their assignment are summarized in Tables 1 and 2. These data are in agreement with the values reported in the literature for pyoverdin G4R and other pyoverdins with similar structure.[22]

2.2. Peptide Chain Sequence. Sequential assignments of the pyoverdin peptide chain were obtained from the combination of ^{1}H−^{1}H NOESY spectra and ^{1}H−^{13}C and ^{1}H−^{15}N LR-HSQC experiments. In the NOESY spectra, the cross-peak between H11 of the chromophore at 5.605 ppm and the NH resonance of Asp-1 at 8.904 ppm indicates that Asp is bound directly to the chromophore and thus is the first residue of the peptide chain. The presence of $NH_i \rightarrow H\alpha_i$ and $NH_i \rightarrow H\alpha_{i-1}$ cross-peaks was used to establish the connectivities between the neighboring residues. The connectivities were confirmed by the presence of weak $NH_i \rightarrow C\alpha_{i-1}$ and $H\alpha_{i-1} \rightarrow N_i$ cross-peaks in LR-HSQC experiments. The data allowed for unambiguous assignment of the peptide sequence as Asp−Orn−OHAsp−Dab−Gly−Ser−cOHOrn. All of the amino acids identified here are commonly observed in other pyoverdins produced by different *P. putida* strains.[22,27−30] The ^{1}H and ^{13}C chemical shifts are in agreement with those reported earlier for pyoverdin G4R.[22] The ^{1}H chemical shifts at 4.107, 1.990, 1.764, and 3.029 ppm and their respective ^{13}C chemical shifts at 169.13, 51.02, 20.13, and 35.59 ppm assigned to the free form of the Dab (2,4 diaminobutyric acid) moiety are in very good agreement with the chemical shifts at 4.37, 2.09−2.19, and 3.24−3.52 ppm and their respective ^{13}C chemical shifts at 162.5, 52.44, 21.59, and 37.54 ppm determined for the cyclic Dab moiety of pyoverdin G4R.[22]

2.3. Mass Spectrometry. The chromophore structure and amino acid sequence of pyoverdin deduced from NMR data are consistent with the fragment ions obtained by mass spectrometry performed on both unlabeled and ^{15}N-labeled pyoverdin (Table 3). The mass spectrum of pyoverdin obtained by MALDI−PSD analysis shows a molecular ion peak at $m/z = 1092.1$, which is assigned to the parent molecule and a minor peak at (M − 18). The fragment peak observed at $m/z = 357$ and assigned to the chromophore cleaved from the peptide chain is followed by a peak at $m/z = 473$, which results from the addition of Asp, the first amino acid. The second amino acid is Orn, identified from the fragment peaks at $m/z = 587$. The peaks at $m/z = 719$ and 818 identify OHAsp and Dab as the following amino acids in the sequence. The remaining amino acids are identified from C-terminal fragments at $m/z = 275$ and 373. Their equivalent peaks in the ^{15}N-labeled pyoverdin are shifted to a higher mass depending upon their nitrogen content (Table 3). The structure of pyoverdin determined here through NMR and mass spectrometry analysis is identical to the pyoverdin purified from extracts of *P. putida* G4R.[22] However, the pyoverdin reported here contains the free form of Dab (2,4-diaminobutyric acid) instead of the cyclic form (3,4-tetrahydropyrimidine) reported for pyoverdin G4R (Figure 1).

3. Spectrophotometric and Potentiometric Characterization of Pyoverdin. The structure of pyoverdin (Figure 1) shows that this natural siderophore has nine (de)-protonation sites. Five deprotonation sites are within the three bidentate chelating units involved in iron binding, three sites from aspartic acid, ornithine, and Dab in the peptidic chain, and a succinic acid group on the side chain attached to the chromophore. By taking into account the positive charge of the chromophore, the fully deprotonated pyoverdin is denoted L^{5-}. The deprotonation of the hydroxyl of the central α-hydroxycarboxylic acid group pK_a0, which occurs above the pH accessible in potentiometric titrations, was not determined.

The pyoverdin deprotonation constants K_{an} ($n = 1-8$), defined by the equilibrium eqs 1 and 2 are listed in Table 4.

$$LH_{8-n}^{+3-n} \rightleftharpoons LH_{7-n}^{+2-n} + H^{+} \quad (1)$$

$$K_{an} = \frac{[LH_{7-n}^{+2-n}][H^{+}]}{[LH_{8-n}^{+3-n}]} \quad (2)$$

The electronic absorption spectrum of pyoverdin shows two buffer regions between pH 3.50 and 13.50. The first set of spectra recorded from pH 3.50 to 8.50 shows a progressive shift of the absorbance band at 377−400 nm (Figure 2A). These spectral changes were reversible when the solution was titrated from high to low pH. These spectral variations are attributed to the first deprotonation of the chatecholate group of the 2,3-diamino-6,7-dihydroxyquinoline chromophore. The value of the deprotonation constant determined

(27) Budzikiewicz, H.; Fernandez, D. U.; Fuchs, R.; Michalke, R.; Taraz, K.; Rungiviriachai, C. *Z. Naturforsch., C: J. Biosci.* **1999**, *54*, 1021−1026.
(28) Gwose, I.; Taraz, K. *Z. Naturforsch., C: J. Biosci.* **1992**, *47*, 487−502.
(29) Persmark, M.; Frejd, T.; Mattiasson, B. *Biochemistry* **1990**, *29*, 7348−7356.
(30) Sultana, R.; Siddiqui, B. S.; Taraz, K.; Budzikiewicz, H.; Meyer, J. M. *Tetrahedron* **2001**, *57*, 1019−1023.

Table 4. Deprotonation Constants for Free Pyoverdin[a]

equilibria	thermodynamic constant
$LH^{4-} \rightleftharpoons L^{5-} + H^+$	$pK_{a1} = 12.88^b \pm 0.30$ 10.8^c
$LH_2^{3-} \rightleftharpoons LH^{4-} + H^+$	$pK_{a2} = 10.24 \pm 0.40$
$LH_3^{2-} \rightleftharpoons LH_2^{3-} + H^+$	$pK_{a3} = 9.56 \pm 0.30$
$LH_4^{-} \rightleftharpoons LH_3^{2-} + H^+$	$pK_{a4} = 8.12 \pm 0.30$ 8.4^c
$LH_5 \rightleftharpoons LH_4^{-} + H^+$	$pK_{a5} = 6.40 \pm 0.30$ $6.35^b \pm 0.15$ 5.7^c 6.4^c
$LH_6^{+} \rightleftharpoons LH_5 + H^+$	$pK_{a6} = 4.97 \pm 0.40$ 4.8^c
$LH_7^{2+} \rightleftharpoons LH_6^{+} + H^+$	$pK_{a7} = 3.48 \pm 0.11$
$LH_8^{3+} \rightleftharpoons LH_7^{2+} + H^+$	$pK_{a8} = 2.72 \pm 0.16$ 3.0^c

[a] Conditions: $T = 298$ K and $I = 0.10$ M $NaNO_3$. ± Refer to the standard deviation. [b] Determined from spectrophotometric measurements. [c] References 15 and 16.

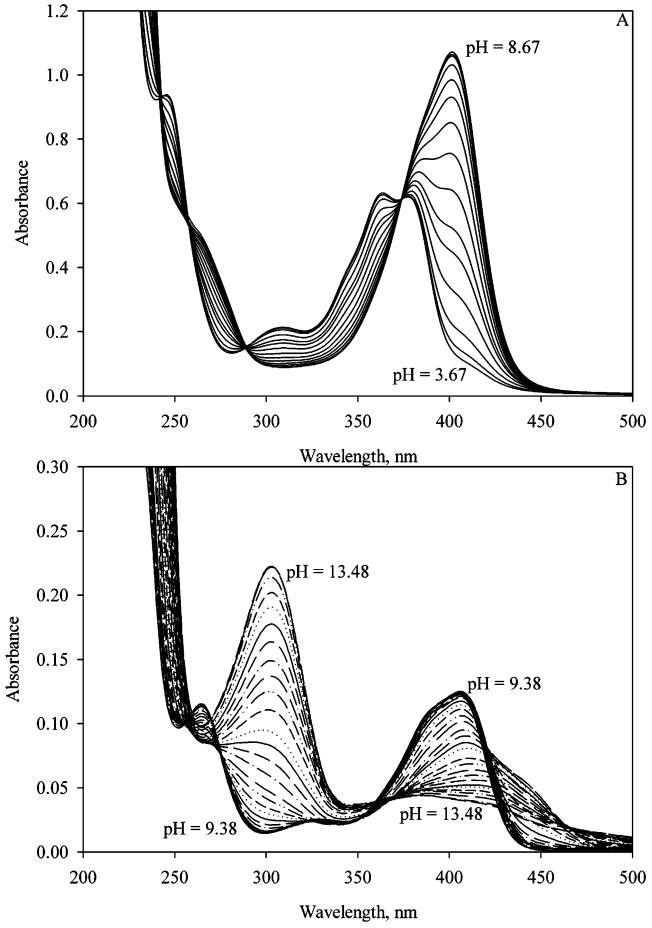

Figure 2. Spectrophotometric titration of metal-free pyoverdin as a function of pH at $I = 0.10$ M ($NaNO_3$) and $T = 298$ K. Conditions: (A) [pyoverdin] $= 0.055 \times 10^{-3}$ M, pH was varied from 3.67 to 8.67. (B) [pyoverdin] $= 0.0075 \times 10^{-3}$ M, pH was varied from 9.38 to 13.48. pH values above 11 were calculated on the basis of the amount of base added.

from numerical analysis of the spectral data is $pK_{a5} = 6.35$. The second buffer region is observed between pH 9.56 and 13.5. The variation of the absorption spectra in this pH domain shows a decrease in the absorbance band at 400 nm accompanied with the appearance of a new absorbance band at 300 nm (Figure 2B). These spectral variations are attributed to the second deprotonation of the chatecholate

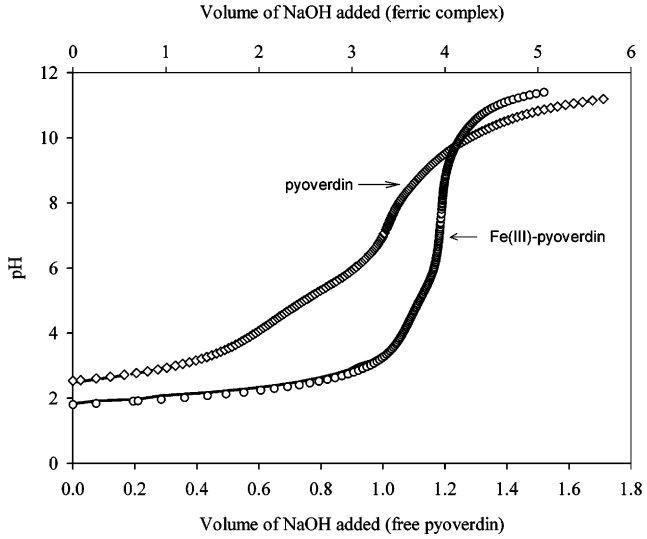

Figure 3. Potentiometric titration of pyoverdin and the Fe(III)−pyoverdin complex. Conditions: [NaOH] = 0.1014 M, $I = 0.10$ M ($NaNO_3$), $T = 298$ K. Pyoverdin titration: [pyoverdin] $= 0.0199 \times 10^{-3}$ M; Fe(III)−pyoverdin titration: [pyoverdin] $= 0.0208 \times 10^{-3}$ M; [Fe(III)] $= 0.0208 \times 10^{-3}$ M. The symbols (diamonds and circles) represent the experimental data points, and the solid lines the numerical fit obtained using refined parameters.

group of the 2,3-diamino-6,7-dihydroxyquinoline chromophore. At very high pH (>13), the catecholate chromophore oxidizes in air, making the spectral changes irreversible, which decreases the accuracy of the deprotonation constant determined for this group. However, the extent of the oxidation was insignificant over the duration of the spectrophotometric titration. The spectral changes attributed to the second deprotonation of the chromophore were not previously reported. The pK_a value determined from numerical analysis of the spectral data between pH 9.56 and 13.5 is $pK_{a1} = 12.88$. This value is greater than the value determined in previous studies ($pK_a = 10.80$[15,16]). The structure of the pyoverdin chromophore examined here is closely related to the chromophores of the two pyoverdins examined previously and it is unlikely that the small differences in the chromophore structure would be responsible for the large differences in the deprotonation constant observed. Although, the pK_a values ($pK_a = 10.80$[15,16]) reported previously are within the range determined for other catecholate groups ranging from 10.8 to 13,[31,32] it is likely that previous studies did not examine the ligand in the pH domain where the second deprotonation of the ligand occurs.

The potentiometric titration of pyoverdin in the pH range 2.54−11.19 shows several deprotonations (Figure 3). The color of the pyoverdin solution changes from pale yellow in very acidic media (pH < 2.5) to a fluorescent green-yellow above neutral pH. Under our experimental conditions, no precipitation was observed through the entire pH range. Seven deprotonation constants were determined from numerical analysis of the data. The deprotonation constants of

(31) Rodgers, S. J.; Lee, C.-W.; Ng, C. Y.; Raymond, K. N. *Inorg. Chem.* **1987**, *26*, 1622−1625.
(32) Raymond, K. N.; Muller, G.; Matzanke, B. F. In *Topics in Current Chemistry*; Boschk, F. L., Ed.; Springer-Verlag: Berlin, 1984; Vol. 123, pp 50−97.

the amine groups of ornithine and Dab are expected to be very close to each other, limiting the accuracy of the determination of the individual deprotonation constants for these two groups. The average pK_a computed for these two deprotonation sites, p$K_{a2,3}$ = 9.9, is in very good agreement with literature values for the deprotonation of NH_3^+ groups for side chains on free amino acids (pK_a = 10.1−10.75 for ornithine[33]). Their individual pK_a's were determined to be pK_{a2} = 10.24 for ornithine, in agreement with the data available in the literature for ornithine, and pK_{a3} = 9.56, assigned to Dab. The next pK_a, pK_{a4} = 8.12, is assigned to the deprotonation of the hydroxamic acid group. This value falls within the range of values measured for hydroxamic acids, 7.5−9.8.[34,35] The following deprotonation, pK_{a5} = 6.40, is assigned to the first deprotonation of the catecholate group, in agreement with the value obtained from spectrophotometric titration (pK_{a5} = 6.35). This value compares well with previously reported values that range from 5.7 to 6.4.[15,16] The deprotonation constant, pK_{a6} = 4.97 is assigned to the deprotonation of the succinic acid side chain attached to the chromophore. This assignment is based on the values available in the literature for succinic acid that range from pK_a = 5.08−5.66.[33,36] The two remaining deprotonation constants K_{a7} and K_{a8} are assigned to the deprotonation of the carboxylic acid groups. The value of pK_{a7} = 3.48 is assigned to the aspartic acid group present on the peptidic chain, which compares well with the value of 3.70 for aspartic acid.[33] The value of pK_{a8} = 2.72 is assigned to the central α-hydroxycarboxylic acid, which is within the range determined for similar carboxylic acid groups.[16] The deprotonations of these two carboxylic groups are not well separated, limiting the accuracy of the individual constants.

The deprotonation constants presented in Table 4 and the spectrophotometric titrations (Figure 2A and B) suggest that the species LH_8^{3+}, LH_7^{2+}, and LH_6^+ have indistinguishable UV−visible absorption spectra. The spectrum has an absorbance band at 365 nm and a shoulder at 377 nm. The extinction coefficient ϵ_{377} = 12 670 M^{-1} cm^{-1} for the free pyoverdin at pH 5.0 was determined from an aqueous solution whose iron concentration was measured using a graphite furnace atomic absorption spectrometer (GFAA). The species LH_5, LH_4^{1-}, LH_3^{2-}, LH_2^{3-}, and LH^{4-} that form at higher pH also have indistinguishable UV−visible spectra. The spectrum is characterized by an intense absorbance band at 401 nm with an extinction coefficient ϵ_{401} = 22180 M^{-1} cm^{-1} at pH 9. The fully deprotonated pyoverdin, which is not stable and oxidizes in air, is characterized by an absorbance band at 303 nm.

Iron(III)−Pyoverdin Complex Formation and Deprotonation Constants. The spectrophotometric titration of the Fe(III)−pyoverdin complex over the pH range 1.0−7.5 shows a progressive shift in the absorbance band at 377 to lower energy upon pH increase (Figure 4 A and B). These changes occur at lower pH for the ferric complex than observed for the free ligand, as expected. The spectral changes recorded in this pH range also show a broad ligand-to-metal charge transfer band at higher wavelength (>420 nm, not observed in the ligand only spectrum) (Figure 2A). The intensity of this band increases with pH up to pH 7. The spectral data do not contain subsets of spectra with clear isosbestic points, indicating that several species are formed in this pH range. These data indicate that the ferric complex forms at very low pH (<2) and undergoes sequential deprotonations. The spectrophotometric data obtained over the pH range between 1.0 and 2.0, where the initial changes were observed (Figure 4A), were analyzed numerically to determine the thermodynamic formation constant log β_{FeLH6}

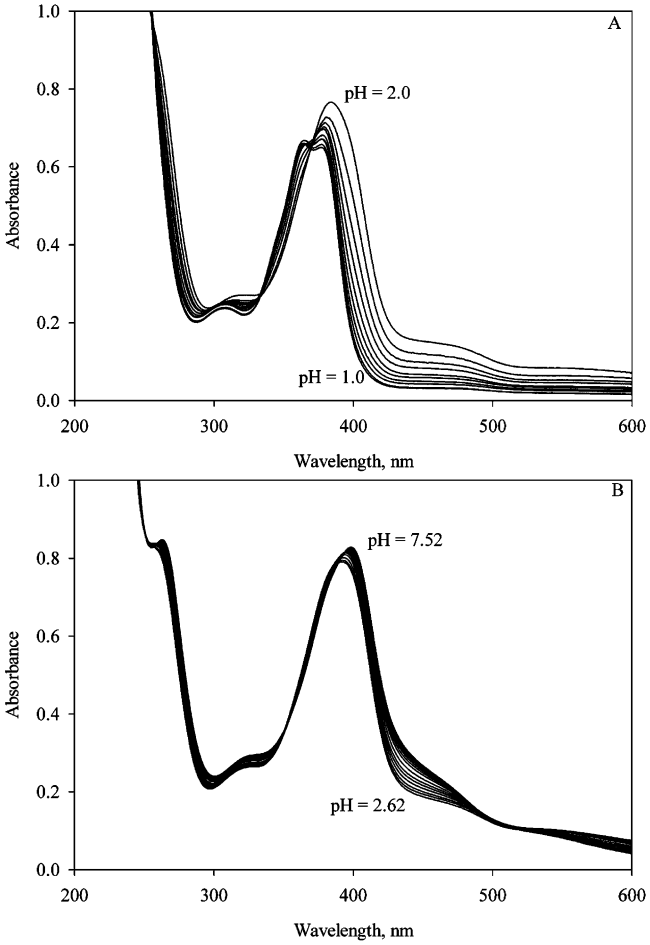

Figure 4. Spectrophotometric titration of Fe(III)−pyoverdin as a function of pH at I = 0.10 M ($NaNO_3$) and T = 298 K. [Fe(III)−pyoverdin] = 0.055 × 10^{-3} M. (A) pH was increased from 1.0 to 2.0; (B) pH was increased from 2.62 to 7.52.

(33) Martell, A. E.; Smith, R. M. *Critical Stability Constants*; Plenum Press: New York and London, 1989; Vol. 4.
(34) Monzyk, B.; Crumbliss, A. L. *J. Org. Chem.* **1980**, *45*, 4670−4675.
(35) Brink, C. P.; Fish, L. L.; Crumbliss, A. L. *J. Org. Chem.* **1985**, *50*, 2277−2281.
(36) Ivaska, A. *Talanta* **1974**, *21*, 1175−1181.
(37) Wawrousek, E. F.; McArdle, J. V. *J. Inorg. Biochem.* **1982**, *17*, 169−183.
(38) Wong, G. B.; Kappel, M. J.; Raymond, K. N.; Matzanke, B.; Winkelmann, G. *J. Am. Chem. Soc.* **1983**, *105*, 810−815.
(39) Anderegg, G.; L'Eplattenier, F.; Schwarzenbach, G. *Helv. Chim. Acta*, **1963**, *46*, 1409−1422.
(40) Loomis, L. D.; Raymond, K. N. *Inorg. Chem.* **1991**, *30*, 906−911.
(41) Lee, C. W.; Ecker, D. J.; Raymond, K. N. *J. Am. Chem. Soc.* **1985**, *107*, 6920−6923.
(42) Dhungana, S.; Miller, M. J.; Dong, L.; Ratledge, C.; Crumbliss, A. L. *J. Am. Chem. Soc.* **2003**, *125*, 7654−7663.
(43) Spasojevic, I.; Armstrong, S. K.; Brickman, T. J.; Crumbliss, A. L. *Inorg. Chem.* **1999**, *38*, 449−454.

Table 5. Stability Constants of the Ferric Complex of Pyoverdin

equilibria	thermodynamic values	pK_{an}^{Fe}	*n*
$L^{5-} + Fe^{3+} - H^{+} \rightleftharpoons LFe-H^{3-}$	$\log \beta_{FeL-H} = 20.71 \pm 0.05$	10.35	1
$L^{5-} + Fe^{3+} \rightleftharpoons LFe^{2-}$	$\log \beta_{FeL} = 31.06 \pm 0.04$	9.17	2
$L^{5-} + H^{+} + Fe^{3+} \rightleftharpoons LHFe^{-}$	$\log \beta_{FeLH} = 40.23 \pm 0.30$	5.74	3
$L^{5-} + 2H^{+} + Fe^{3+} \rightleftharpoons LH_2Fe$	$\log \beta_{FeLH2} = 45.97 \pm 0.30$	4.71	4
$L^{5-} + 3H^{+} + Fe^{3+} \rightleftharpoons LH_3Fe^{+}$	$\log \beta_{FeLH3} = 50.68 \pm 0.30$	3.73	5
$L^{5-} + 4H^{+} + Fe^{3+} \rightleftharpoons LH_4Fe^{2+}$	$\log \beta_{FeLH4} = 54.41 \pm 0.33$	2.91	6
$L^{5-} + 5H^{+} + Fe^{3+} \rightleftharpoons LH_5Fe^{3+}$	$\log \beta_{FeLH5} = 57.32 \pm 0.22$	2.71	7
$L^{5-} + 6H^{+} + Fe^{3+} \rightleftharpoons LH_6Fe^{4+}$	$\log \beta_{FeLH6} = 60.03 \pm 0.22$[a]		

[a] Determined from nonlinear least-squares analysis of spectrophotometric data.

= 60.03 (Table 5). The formation of this complex results in a decrease in the absorbance band at 365 and an increase of the absorbance band at 377 nm. The formation of this complex occurs below the pH domain accessible to potentiometric titration, and therefore, the value could not be determined potentiometrically. At pH 1.80, the start of the potentiometric titration, the fraction of free iron concentration present is too small to allow for the refinement of the overall formation constant from the potentiometric titration alone. However, by using the value of the overall formation constant $\log \beta_{FeLH6} = 60.03$ determined from spectrophotometric measurements, the sequential deprotonation constants of the ferric−pyoverdin complex were calculated from potentiometric titration data (Figure 3). The values of $\log \beta_{FeH6L}$ and the pyoverdin deprotonation were fixed at the values listed in Table 4 to refine the remaining constants. The resulting calculated stability constants are listed in Table 5. The chelation of Fe(III) by pyoverdin and the subsequent stepwise deprotonation of the complex formed are summarized in Scheme 1. The deprotonation sequence determined from the assignment of the different pK_a's is consistent with previous kinetics dissociation studies, the pK_a's of functional groups in the free ligand, and with known relative binding strengths of individual Fe(III) chelators (hydroxamate > catecholate > α-hydroxycarboxylic acid).[16]

The pK_a values of the protonation sites of the ferric complex not involved in metal chelation differ slightly from their values in the free ligand, as expected. By comparing to the pK_a values of the free ligand (pK_{a2} = 10.24, pK_{a3} = 9.56), the pK_a values of the ferric complex $pK_{a1}^{Fe} = 10.35$ and $pK_{a2}^{Fe} = 9.17$ were assigned to the protonation sites of the free amine groups in ornithine and Dab. The average value (9.76) is in agreement with the average pK_a value determined for the free ligand (9.90). The value of $pK_{a4}^{Fe} = 4.71$ is assigned to the succinic acid group. This value compares well with pK_{a6} = 4.97 determined for this protonation site in the free ligand.

The α-hydroxy acid moiety is a less powerful chelating group than hydroxamate and catecholate. It has been shown through kinetic dissociation studies to be the last moiety to coordinate iron.[16] Therefore, the pK_{a3}^{Fe} value of 5.74 determined from potentiometric measurements is assigned to the proton release from the hydroxyl group of the α-hydroxy acid moiety upon iron chelation. The pK_a value of the carboxylic acid in the free ligand, pK_{a8} = 2.72, is expected to remain unchanged and is therefore assigned the value of $pK_{a1}^{Fe} = 2.71$. The assignment of the remaining pK_a values is more difficult since these values are close to each other. The

Scheme 1. Chelation of Fe(III) by Pyoverdin and Subsequent Stepwise Deprotonations of the Fe(III) Complex.

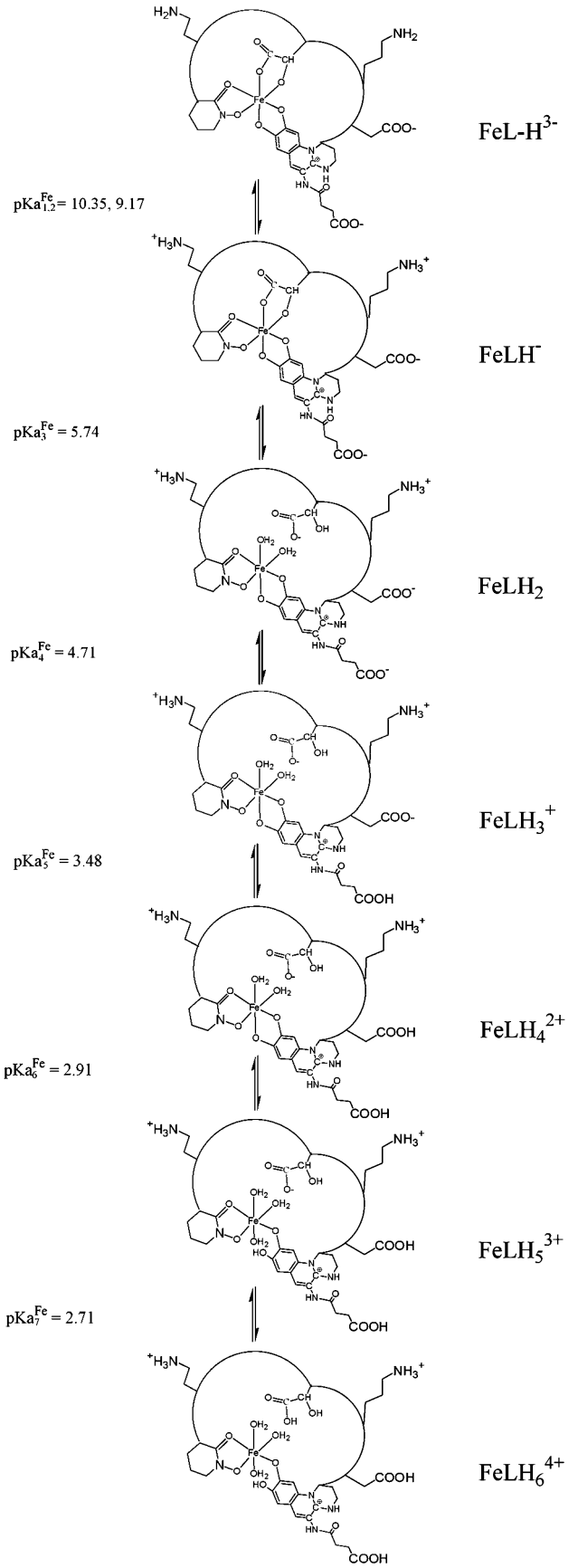

Table 6. Redox Potentials of Fe(III)−Siderophore Complexes

siderophore	$E_{1/2}$ (V) (NHE)[a]	pFe[b]	$\log \beta_{Fe(III)-L} - \log \beta_{Fe(II)-L}$	ref
pyoverdin	−0.480	25.13	21.1	this work
azotobactin δ	−0.390	20.37[c]	19.6	16
pyoverdin PaA	−0.510	27	21.6	15
desferrichrome	−0.400	25.2	19.8	37−39
enterobactin	−0.750	35.5	25.7	40, 41
exochelin MN	−0.595	31.1	23.1	42
desferrioxamine B	−0.482	26.6	20.9	43

[a] Redox potentials independent of pH. [b] Defined as $-\log [Fe^{3+}]$ at $[Fe(III)]_{tot} = 10^{-6}$ M, $[ligand]_{tot} = 10^{-5}$ M, and pH = 7.4. [c] Calculated from the data given in ref 16.

deprotonation constant of the ferric−pyoverdin complex ($\log \beta_{FeLH4} - \log \beta_{FeLH3} = 3.73$) is tentatively assigned to the deprotonation of the aspartic acid group, which does not participate in iron coordination. This value compares favorably with the $pK_{a7} = 3.48$ determined for the aspartic acid group in the free pyoverdin. The value of the deprotonation constant ($\log \beta_{FeLH5} - \log \beta_{FeLH4} = 2.91$) is assigned to the proton released upon Fe(III) coordination by the catecholate group (Scheme 1).

The initial charge-transfer band observed at higher wavelength (>500 nm) in the pH domain 1.0−2.0 (Figure 4A) can be assigned to the Fe(III) coordination by the hydroxamate moiety by comparison with the classical values of the charge-transfer band displayed upon the formation of Fe(III)−monohydroxamate complexes which are centered at around 510 nm. Within the same pH domain the increase in the absorbance at wavelengths >420 nm can be assigned to the formation of the Fe(III)−catecholate complex.

The pM (defined as $-\log [Fe^{3+}]$ at $[Fe(III)]_{tot} = 10^{-6}$ M, $[ligand]_{tot} = 10^{-5}$ M, and pH = 7.4) value of pyoverdin, calculated from the deprotonation constants and the iron binding constants (Tables 3 and 4) is 25.13. This value is within the range of pM values determined for natural siderophores (Table 6), indicating strong binding affinities for Fe(III). The value determined here for pyoverdin is slightly smaller than the pM value of 27 determined for pyoverdin PaA.[15] The difference in the Fe(III) binding affinity of pyoverdin PaA and the pyoverdin examined here is related to the binding groups involved in Fe(III) chelation. Pyoverdin PaA, which chelates the Fe(III) by a catecholate and two hydroxamate groups, is a stronger chelator than is the pyoverdin examined here, which chelates iron by a catecholate, a hydroxamate, and a α-hydroxycarboxylic group.

Electrochemical Reduction. The redox properties of the Fe(III/II)−pyoverdin complex were examined by cyclic voltammetry performed on a relatively concentrated solution of the complex (2.0 mM) prepared with slight excess of pyoverdin over iron (pyoverdin/iron = 1.2). The ionic strength was kept constant at 0.10 M by the addition of $NaNO_3$. The recorded cyclic voltammograms display strong pH dependence. In acidic solution (pH < 3), the cyclic voltammograms were irreversible, with a large peak-to-peak separation and a very small reoxidation wave. At higher pH (∼pH 3.5−8), where the Fe−pyoverdin complex is present as a mixture of several protonated species, the cyclic voltammograms are reversible but redox potential varies significantly with pH. The cyclic voltammogram (Figure 5) recorded at pH 4.99 shows a quasi-reversible couple with peak-to-peak separation of 95 mV and a reduction potential at −0.395 V. The measured redox potential becomes independent of the pH over a narrow pH range (∼pH 9−11) where the coordination of Fe by pyoverdin is hexadentate. In this pH range, the reduction potential corresponding to the Fe(III/II)−pyoverdin was determined to be $E_{1/2} = -0.480$ V (NHE). The strong negative value measured for the reduction potential of the Fe(III/II)−pyoverdin complex is within the range observed for natural siderophores (Table 6). The negative redox potential of iron−siderophore complexes is a direct result of the high affinity of siderophores toward Fe(III) binding and their selectivity for Fe(III) over Fe(II). The difference in Fe(III) versus Fe(II) binding calculated for pyoverdin using eq 3 is within the range of other natural siderophores.

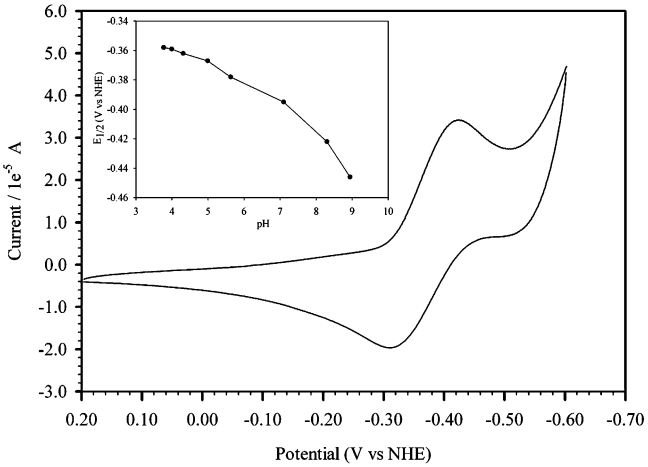

Figure 5. Cyclic voltammogram of the Fe(III)−pyoverdin complex recorded using a three electrode cell. Conditions: [Fe(III)−pyoverdin] = 2.0×10^{-3} M, pH = 4.99, $I = 0.10$ M ($NaNO_3$), scan rate 60 mV/s, $T = 298$ K. $E_{1/2} = -0.367$ V (vs NHE) with peak-to-peak separation of 96 mV. The inset shows the variation of reduction potential ($E_{1/2}$) of the complex Fe(III)−pyoverdin as a function of pH.

$$\log(\beta_{Fe(III)-siderophore}) - \log(\beta_{Fe(II)-siderophore}) = (E^0_{Fe} - E^0_{Fe(III/II)-siderophore})/0.059 \quad (3)$$

The large difference between Fe(III) and Fe(II) binding, which is observed for all siderophores, is a key to iron release from siderophores. In addition to the difference in siderophore binding affinity for Fe(III) versus Fe(II), all Fe(II) siderophore complexes undergo protonations at higher pH's relative to Fe(III)−siderophore complexes. This susceptibility to protonation contributes to the pH dependence of the observed redox potential. The redox potential of the Fe(III/II)−pyoverdin complex shifts more positive as the pH is lowered (Figure 5 inset). This gradual shift is mainly the result of the protonation of the Fe(II)−pyoverdin complex. This trend is observed for almost all siderophores and supports the thesis that iron is released from siderophores through a reduction process followed by acid dechelation and iron exchange.[2]

Summary and Conclusions

The siderophore produced by *P. putida* strain ATCC 33015 was purified and its structure characterized by mass spectrometry (MALDI-TOF−PSD) and several multinuclear 2-D NMR techniques. The molecular structure of the pyoverdin siderophore produced by this bacterium is similar to a previously characterized pyoverdin produced by *P. putida* G4R.[22] The structure comprises a chromophore group derived from 2,3-diamino-6,7-dihydroxyquinoline with an iron-binding catecholate functional group and a peptide chain with the following amino acids: Asp−Orn−OHAsp−Dab−Gly−Ser−cOHOrn. The two remaining bidentate functional groups involved in iron chelation are a hydroxamate group at the end of the peptidic chain and an α-hydroxycarboxylic group in the middle of the peptidic chain. The deprotonation constants of free pyoverdin and its Fe(III) chelation properties were determined by potentiometric and spectrophotometric measurements, and the redox properties of the Fe(III)−pyoverdin complex were studied by cyclic voltammetry. Pyoverdin binds iron in very acidic media through its hydroxamate binding group but does not fully coordinate Fe(III) until neutral pH. The thermodynamic properties of the ferric−pyoverdin complex are similar to the properties of other natural siderophores. Pyoverdin has a high and selective binding affinity for Fe(III) and a low affinity for Fe(II). In addition, all Fe(II)−siderophore complexes tend to undergo proton driven dissociations at relatively high pH. These properties support the mechanism of iron release from siderophores that involves the reduction of the Fe(III)−siderophore complex. The redox potential of Fe(III)−pyoverdin at physiological pH, $E_{1/2} = -0.395$ V, is accessible to bacterial reductants, which can reduce the Fe(III)−pyoverdin complex to a more labile and thermodynamically weaker Fe(II)−pyoverdin complex, providing a path for iron utilization within the cell.

Acknowledgment. We gratefully acknowledge financial support from the nuclear attributions program (NA-22) exploratory research program, and the Environmental Remediation Sciences Program, Office of Biological and Environmental Research, Office of Science, of the U.S. Department of Energy. We thank Dr. Larry Hersman, Dr. Christy Ruggiero, and Mr. Joe Lack for the use of their HPLC instrument and other assistance.

IC060196P